analogous iron complex and the free olefin): δ 1.74, H^{1a} (2.20, 5.35); 2.47, H^{1b} (2.75, 6.35); 2.81, H^{1c} (3.08, 5.95); 3.29, H^2 (3.41, 3.49); J_{gem} = 3.0 Hz, J_{cis} = 8.1 Hz, J_{trans} = 11.1 Hz; in toluene-d_8 at -40 °C (and ambient temperature, respectively). UV-visible data: 268 nm (max, ε ≈ 7000), in hexane which contains 0.5% methyl acrylate; the same solution was used in the reference cell.

2b. A 0.19-g sample of $Ru_3(CO)_{12}$ (0.3 mmol) and 0.13 g of dimethyl fumarate (0.9 mmol) gave 0.19 g of **2b** (59%), mp 101-102 °C. Anal. Calcd for $C_{10}H_8O_8Ru$: C, 33.61; H, 2.26; Ru, 28.29. Found: C, 33.40; H, 2.08; Ru, 28.48. The mass spectrum shows prominent peaks (^{102}Ru containing fragments) at *m/e* 330, 302, 274, and 246 ($M^+ - nCO$, *n* = 1-4), 327 ($M^+ - OCH_3$) and further fragmentation products at *m/e* 216, 188, 158, 130, and 102. ^1H NMR data: δ 3.73, H^1 (3.83, 6.86); 3.33, H^2 (3.35, 3.31); in benzene-d_6 at ambient temperature. UV-visible data: ~295 (wsh, ε = 4350), ~250 (sh, ε = 9100), 227 nm (ε = 9950).

2c. A 0.19-g sample of $Ru_3(CO)_{12}$ (0.3 mmol) and 0.13 g of dimethyl maleate (0.9 mmol) gave 0.29 g of **2c** (90%), mp 45-45.5 °C. Anal. Calcd for $C_{10}H_8O_8Ru$: C, 33.61; H, 2.26; Ru, 28.29. Found: C, 33.98; H, 2.06; Ru, 27.98. The mass spectrum is similar to that of **2b**. ^1H NMR data: δ 3.05, H^1 (3.09, 5.96); 3.48, H^2 (3.41, 3.46); in benzene-d_6 at ambient temperature. UV-visible data: ~250 (wsh, ε = 7150), 226 nm (ε = 9150).

2d and **2f** have been isolated by a similar procedure as white solids; however, due to the instability of these compounds yields could not be accurately determined, and physical data other than CO stretching frequencies (Table I) are still lacking.

Quantum Yield Determinations. Quantum yields (reproducible within ±5%) were determined by using an electronically integrating actinometer which was calibrated by ferrioxalate actinometry.[32] The actinometer has been described elsewhere[33] and compensates for incomplete absorption of light in the sample cell. All experiments were carried out at 298 ± 1 K in degassed hexane solutions containing ~2.2×10^{-4} M $Ru_3(CO)_{12}$. Irradiations at 313 or 395 nm were performed in quartz cuvettes (*d* = 1 cm), using a Hanovia 1000 W Hg-Xe lamp in connection with a Schoeffel Instruments GM 250 single-grating monochromator. Light intensities were in the order of 10^{-6}-10^{-5} E min^{-1}. Disappearance of $Ru_3(CO)_{12}$ was monitored by measuring the absorption at the 390-nm maximum. Constant ϕ_{-1} values were obtained at both wavelengths, 313 and 395 nm, over a wide range of conversion (up to 40%). At 313 nm appropriate corrections were made in order to account for internal light filter effects due to the tail absorptions of **2a** and **2b**. The following ε values (1 mol^{-1} cm^{-1}) were used: ε[$Ru_3(CO)_{12}$] = 7360 at 390 nm (values reported in the literature are 7700[4] and 6400[23]) and 9300 at 313 nm; ε (**2a**) = 2240 and ε (**2b**) = 2380 at 313 nm.

Acknowledgment. We wish to thank the staff of the spectroscopic laboratories for their help and Herrn K. Schneider for experimental assistance. J.T. is indebted to the Alexander von Humboldt Foundation for support of this research by a fellowship during his stay at the Institut für Strahlenchemie in 1978/1979.

(32) Hatchard, C. G.; Parker, C. A. *Proc. R. Soc. London, Ser. A* **1956**, *235*, 518. Murov, S. L. in "Handbook of Photochemistry"; Marcel Dekker: New York, 1976; p 119.
(33) Amrein, W.; Gloor, J.; Schaffner, K. *Chimia* **1974**, *28*, 185.

The Synthesis, Redox Properties, and Ligand Binding of Heterobinuclear Transition-Metal Macrocyclic Ligand Complexes. Measurement of an Apparent Delocalization Energy in a Mixed-Valent Cu^ICu^{II} Complex

R. R. Gagné,*[1] C. L. Spiro,[1] T. J. Smith,[2] C. A. Hamann,[1] W. R. Thies,[2] and A. K. Shiemke[2]

Contribution No. 6276 from the Division of Chemistry and Chemical Engineering, California Institute of Technology, Pasadena, California 91125. *Received August 4, 1980*

Abstract: A series of binuclear complexes $M_A^{II}M_B^{II}L^{2+}$ have been synthesized and characterized. The binucleating macrocyclic ligand L^{2-} is a symmetric Schiff base derived by condensing 2 equiv of 2,6-diformyl-4-methylphenol with 2 equiv of 1,3-diaminopropane, resulting in two identical N_2O_2 coordination sites. In all cases, $M_A(II)$ = Cu(II) while M_B was varied across the series $M_B(II)$ = Mn(II), Fe(II), Co(II), Ni(II), Cu(II), and Zn(II). The electrochemical properties of these species were examined by cyclic voltammetry, differential pulse polarography, sampled DC polarography, and coulometry. In each case reversible to quasi-reversible Cu(II)Cu(I) electrochemistry was observed. The Cu(II)Cu(I) reduction potential was, within experimental error, invariant with respect to the remote metal M_B; E_f(Cu(II)Cu(I)) = -1.068 V vs. ferrocene/ferrocinium(1+). The one exception is the homobinuclear complex $M_A(II) = M_B(II)$ = Cu(II); the homobinuclear complex was more readily reduced, E^f = -0.925 V vs. Fc/Fc^+, than the heteronuclear species. After a correction due to magnetic stabilization the difference between the heteronuclear and homonuclear reduction potentials, 143 mV = 3.3 kcal/mol, has been ascribed to a special stability associated with the mixed-valent $Cu^{II}Cu^IL^+$ species, where some electronic delocalization has been previously demonstrated. In addition, the electrochemical properties of homonuclear complexes ($M_A = M_B$) are reported. The ligand-binding properties of the species $Cu^IM_B^{II}L^+$, $M_B(II)$ = Mn(II), Fe(II), Co(II), Ni(II), Cu(II), and Zn(II), have been examined. Cu(I) shows an affinity for the axial bases carbon monoxide, ethylene, tris(*o*-methoxyphenyl)phosphine, and 4-ethylpyridine. In contrast to the Cu(II)/Cu(I) reduction potentials, the binding of axial bases to Cu(I) does seem to depend on the nature of the remote metal, M_B.

Multimetallic species occupy an important position in modern inorganic chemistry. They are ubiquitous in nature as active sites in a variety of metalloenzymes and are playing a significant and expanding role in industrial chemical catalysis.

The importance of multimetallic species has prompted a wide range of theoretical treatments concerning their properties. These include orbital models for magnetic exchange coupling,[3] potential energy surface treatments of thermal intramolecular electron

(1) California Institute of Technology.
(2) Kalamazoo College, Kalamazoo, Mich.

(3) P. J. Hay, J. C. Thibeault, and R. Hoffmann, *J. Am. Chem. Soc.*, **97**, 4884 (1975).

0002-7863/81/1503-4073$01.25/0

transfer,[4] and perturbation calculations for optically induced intrasystem charge transfer[4] including vibronic[5] and superexchange[6] coupling contributions.

The experimental study of multimetallic complexes, dating back to 1704 and the discovery of Prussian blue,[7] has not been left fallow. The traditional approach to work in this area has been to synthesize complexes which contain two or more metal ions each with their appropriate complement of external ligands and one or more shared entities referred to as bridging groups. Metal–metal interactions are usually propagated through orbitals on the bridging group in an inner-sphere fashion[8] though outer-sphere through-space coupling is also known.[9] By systematically varying the bridging group and holding the metals and nonbridging ligands constant, scientists have studied the nature and extent of metal–metal communication.

In contrast, our approach has been not to vary the ligands but rather to control as rigorously as possible both the external and bridging groups, while systematically varying the metal ions. This has been accomplished, utilizing complexes of the type **1**,

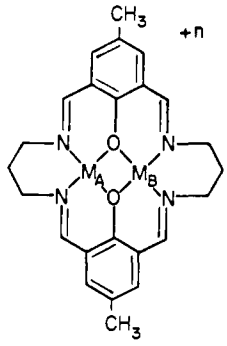

1

$M_AM_BL'^{n+}$. The complexes **1** provide a good opportunity to study metal–metal interactions. By virtue of the close proximity of the metal ions (ca. 3.15 Å)[10-13] the ligand ensures that some intramolecular coupling is likely. In the case of homonuclear species ($M_A = M_B$), originally prepared by Robson and co-workers,[14] the high degree of symmetry requires that the fields and potentials about one metal ion be identical with its adjacent counterpart. This is especially important when comparisons are made to a series of heteronuclear ($M_A \neq M_B$) ions. Our hypothesis is that many differences in the physical, chemical, or redox properties of these complexes can then be ascribed to metal–metal interactions since the liganding environment is held constant. In an earlier communication[15] we reported the redox properties of **1** with copper in the M_A site while M_B was varied across the series M_B = Mn(II), Fe(II), Ni(II), Cu(II), and Zn(II). Since the ligand remains constant, the observed changes in the electrochemical properties at the M_A site have been ascribed to some form of metal–metal communication with the remote metal M_B (vide infra). Reported herein are the detailed syntheses and characterization of these complexes, along with some of the physical, chemical, and redox consequences of these metal–metal interactions.

Scheme I

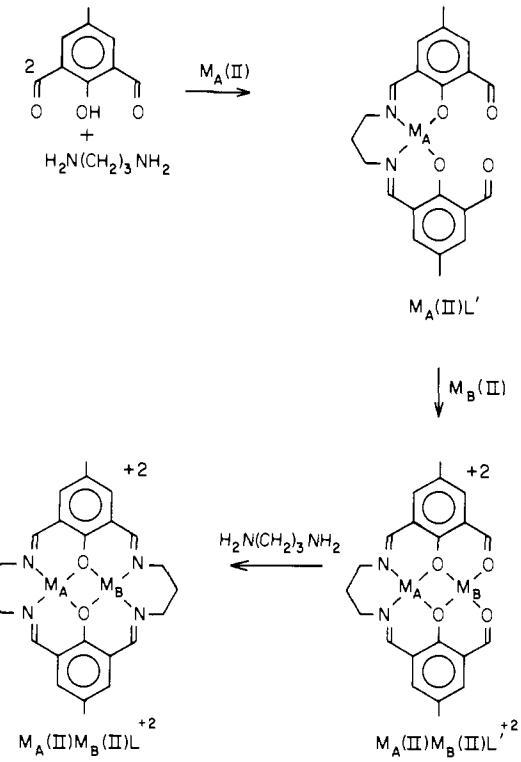

Table I. Absorption Maxima of the Binuclear Macrocyclic Complexes $M_A^{II}M_B^{II}L^{2+}$ [a]

complex	λ_{max}, nm	complex	λ_{max}, nm
$Cu^{II}Mn^{II}L^{2+}$	650	$Cu^{II}Ni^{II}L^{2+}$	625, 775, 1200, 1500
$Cu^{II}Fe^{II}L^{2+}$	600, 1200	$Cu^{II}Cu^{II}L^{2+}$	620[14]
$Cu^{II}Co^{II}L^{2+}$	600, 900	$Cu^{II}Zn^{II}L^{2+}$	610

[a] Spectra were taken in the solid state as Nujol mulls.

Results

Synthesis. Homonuclear complexes ($M_A = M_B$) were prepared by a slight variation of the method of Robson,[14] utilizing a template synthesis. Since we did not succeed in separating mixtures of homo- and heteronuclear species, an alternate pathway to pure mixed-metal binuclear complexes was developed, as outlined in Scheme I. This route was chosen for several reasons. Mononuclear compounds $M_A^{II}L'$ and related systems were prepared and characterized by Okawa and co-workers,[17] who found that the metal ion binds preferentially to the N_2O_2 site. We found that addition of M_B(II) salts to a suspension of $Cu^{II}L'$ in methanol resulted in the rapid complexation of M_B(II) to what is likely the vacant O_4 site. Within 10 min at the ambient temperature formation of crystalline salts of $Cu^{II}M_B^{II}L'^{2+}$ appeared complete. Since the time in solution was short and the temperature apparently too low to surmount the activation barrier to dissociation, little scrambling ($2M_AM_BL'^{2+} \rightleftharpoons M_AM_AL'^{2+} + M_BM_BL'^{2+}$) was observed (vide infra). Subsequent addition of 1 equiv of 1,3-diaminopropane to a solution containing redissolved $Cu^{II}M_B^{II}L'^{2+}$ resulted in the formation[16] of salts of $Cu^{II}M_B^{II}L_2^{+}$ (**1**). It was necessary to isolate the intermediates $Cu^{II}L'$ and $Cu^{II}M_B^{II}L'^{2+}$, as failure to do so resulted in scrambled products. Several attempts at alternate syntheses[18] either by performing reaction sequences

(4) N. S. Hush, *Prog. Inorg. Chem.*, **8**, 391 (1967).
(5) P. N. Schatz, S. B. Piepho, and E. R. Krausz, *Chem. Phys. Lett.*, **65**, 539 (1978).
(6) P. A. Cox, *Chem. Phys. Lett.*, **69**, 340 (1980).
(7) J. Woodward, *Philos. Trans. R. Soc. London* **33**, 15 (1724).
(8) H. Taube, *Ann. N.Y. Acad. Sci.*, **313**, 481 (1978).
(9) B. P. Sullivan and T. J. Meyer, *Inorg. Chem.*, **19**, 752 (1980).
(10) B. F. Hoskins, R. Robson, and G. A. Williams, *Inorg. Chim. Acta*, **16**, 121 (1976).
(11) R. R. Gagné, L. M. Henling, and T. J. Kistenmacher, *Inorg. Chem.*, **19**, 1226 (1980).
(12) B. F. Hoskins, N. J. McLeod, and H. A. Schaap, *Aust. J. Chem.*, **29**, 515 (1976).
(13) C. L. Spiro, S. L. Lambert, T. J. Smith, E. N. Duesler, R. R. Gagné, and D. N. Hendrickson, *Inorg. Chem.*, **20**, 1229 (1981). The Fe–Fe distance is 3.11 Å with both metals constrained to lie in the ligand plane.
(14) N. H. Pilkington and R. Robson, *Aust. J. Chem.*, **23**, 225, (1970).
(15) R. R. Gagné and C. L. Spiro, *J. Am. Chem. Soc.*, **102**, 1443 (1980).
(16) It is noteworthy that this method fails for only one case thus far examined. Addition of 1,3-diaminopropane to $Cu^{II}Ni^{II}L'^{2+}$ does not result in the formation of $Cu^{II}Ni^{II}L^{2+}$ but rather wrests the Ni(II) from the O_4 site, resulting in the reisolation of neutral $Cu^{II}L'$. If the reaction sequence is first carried out by forming $Ni^{II}L'$ with nickel in the N_2O_2 site, with subsequent addition of Cu(II) to form $Ni^{II}Cu^{II}L'^{2+}$, addition of 1,3-diaminopropane does result in the desired product.
(17) H. Okawa and S. Kida, *Bull. Chem. Soc., Jpn.* **45**, 1759 (1972).

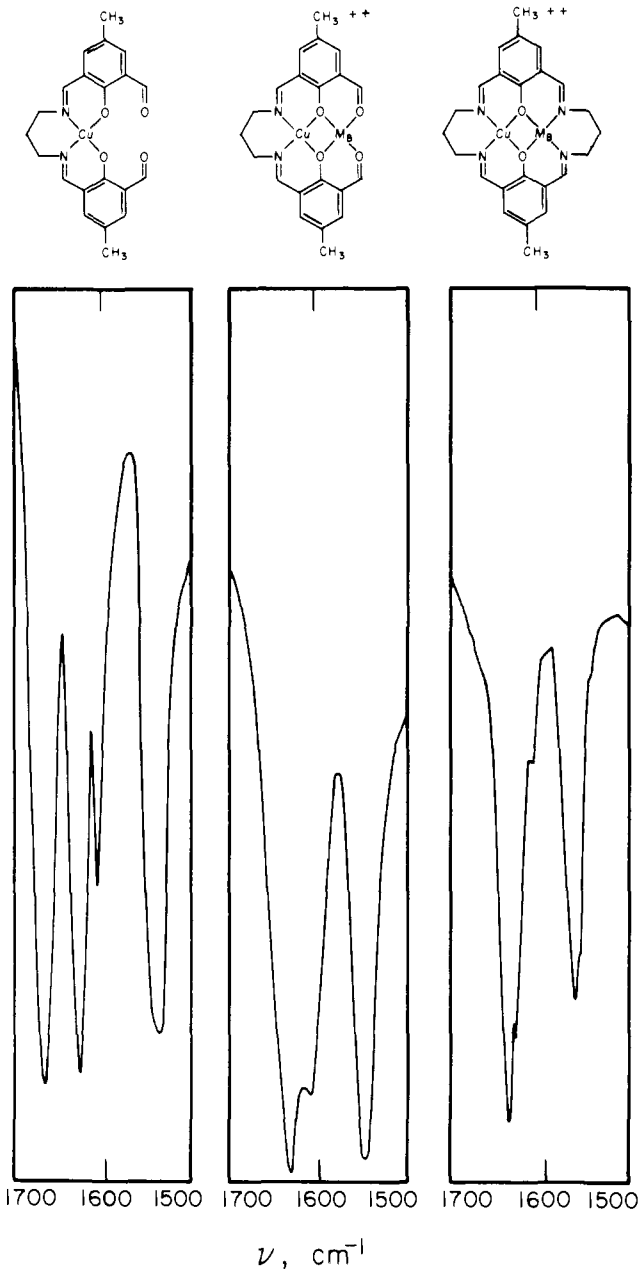

Figure 1. Infrared spectra showing the $\nu_{C=N}$ and $\nu_{C=O}$ stretching frequencies for $Cu^{II}L'$, $Cu^{II}M_B^{II}L'$, and $Cu^{II}M_B^{II}L$.

in situ or by altering the order of reactants consistently resulted in considerable quantities of homonuclear impurities.

Characterization

Spectroscopy. The infrared spectra of all binuclear complexes L are virtually indistinguishable and have been discussed previously.[14] Examination of IR spectra was useful in showing that the formation of complexes of L and its various intermeidates was complete, but it failed to distinguish which metals and in what ratios were present. Figure 1 shows the most diagnostic changes which occur in the various synthetic stages observed in the $\nu_{C=O}$ and $\nu_{C=N}$ stretch region for the compounds $M_A^{II}L'$, $M_A^{II}M_B^{II}L'^{2+}$, and $M_A^{II}M_B^{II}L^{2+}$.

The solid-state electronic absorption spectra of these complexes (Table I) reveals little in the way of metal–metal coupling. It appears that the absorption maxima can be approximated by their homonuclear analogues.[14] The low solubility of these complexes and the presence of intense charge-transfer bands due to the ligand prevented detailed analysis of molar absorptions.

One technique that was useful in characterizing these complexes was X-ray fluorescence spectroscopy. By integration of backscattered X-rays using a scanning electron microscope, metal ratios were approximated and sample homogeneity was confirmed. Though atomic absorption spectroscopy was ultimately utilized in the quantitative determination of metal content in these species, X-ray fluorescence spectroscopy enabled us to discard a large number of impure sample preparations without resorting to more time consuming and expensive analytical procedures.

Magnetic Properties. Room-temperature magnetic moments (Table II) show that each metal is high spin in the solid state. Variable-temperature susceptibility studies[19] indicated some degree of magnetic exchange coupling in the homonuclear complexes. Similar studies on the heteronuclear species are in progress and will be reported elsewhere.[20]

Table II. Room Temperature Magnetic Moments of Binuclear Binuclear Complexes[a]

complex	μ_{eff} (285 K)	complex	μ_{eff} (285 K)
$Cu^{II}Mn^{II}L^{2+}$	4.12	$Cu^{II}Ni^{II}L^{2+}$	1.88
$Cu^{II}Fe^{II}L^{2+}$	3.02	$Cu^{II}Cu^{II}L^{2+}$	0.70[14]
$Cu^{II}Co^{II}L^{2+}$	2.89	$Cu^{II}Zn^{II}L^{2+}$	1.74

[a] All data were taken in the solid state and are corrected for diamagnetism by Pascal's constants. Results are reported on a per metal basis in Bohr magnetons.

Table III. Electrochemical Data for Homonuclear Complexes[a]

compd	solvent	E_1,[b] V vs. Fc	E_2,[b] V vs. Fc
$Mn^{II}Mn^{II}L^{2+}$	methanol	−0.050	+0.065
$Fe^{II}Fe^{II}L^{2+}$	methanol	−0.020	+0.240
$Co^{II}Co^{II}L^{2+}$	methanol	+0.010	+0.240
$Ni^{II}Ni^{II}L^{2+}$	water	+0.080	+0.425
$Cu^{II}Cu^{II}L^{2+}$	methanol	−0.940	*c*
$Cu^{II}Cu^{II}L^{2+}$	DMF[d]	−0.925	−1.310

[a] Measurements were made by differential pulse polarography using a platinum button electrode. Tetrabutylammonium perchlorate (0.1 M) acted as supporting electrolyte in nonaqueous solutions, with sodium bromide (0.1 M) used in water. All redox processes involve (III)/(II) couples excepting the dicopper species, where reductions were observed. [b] An internal reference, the ferrocene/ferricinium(1+) couple, was utilized in all nonaqueous measurements. An internal reference couple, $Ru(NH_3)_6^{3+/2+}$, was utilized in water and calculated vs. ferrocene using an aqueous ferrocene potential of +0.400 V vs. NHE.[22] [c] Solvent reduction occurs prior to $Cu^{II}Cu^{I}L^{+}$ reduction. [d] *N,N*-Dimethylformamide.

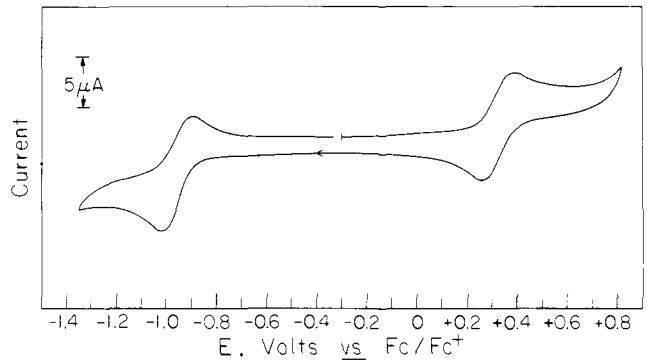

Figure 2. Cyclic voltammogram of $Cu^{II}Mn^{II}L^{2+}$ in methanol. The wave at ~−1 V is the Cu(II)/Cu(I) wave, while the Mn(III)/Mn(II) couple appears at ~+0.3 V. Notice the absence of shoulders which would correspond to homonuclear impurities.

(18) C. Spiro, Doctoral Dissertation, California Institute of Technology, Pasadena, Calif. 1981.

(19) S. L. Lambert and D. N. Hendrickson, *Inorg. Chem.*, **18**, 2683 (1979).

(20) S. L. Lambert, C. L. Spiro, R. R. Gagné, and D. N. Hendrickson, submitted to *Inorg. Chem.* The *J* values for the heteronuclear complexes $Cu^{II}Mn^{II}LCl_2$, $Cu^{II}Fe^{II}LCl_2$, and $Cu^{II}Ni^{II}LCl_2$ are −22.5, −81, and −103 cm^{-1}, respectively. These values enable us to estimate a magnetic contribution to redox parameters as described in the text.

Table IV. Reduction Potentials for the Cu(II)/Cu(I) Couple as a Function of the Remote Metal $M_B(II)$[a]

starting compd	cyclic voltammetry[b]		differential pulse[c] polarography		sampled DC[d] polarography		coulometric[e]	
	E_f, V	$E_{p_a} - E_{p_c}$, V	E_p, V	fwhm, V	$E_{1/2}$, V	slope, V	n value	$E_f(\sigma)$,[b] V
$Cu^{II}Mn^{II}L^{2+}$	−1.080	0.120	−1.070	0.095	−1.052	0.062		−1.070 (10)
$Cu^{II}Fe^{II}L^{2+}$	−1.058	0.060	−1.050	0.095	−1.068	0.062	0.98	−1.063 (12)
$Cu^{II}Co^{II}L^{2+}$	−1.070	0.070	−1.060	0.120	−1.067	0.061		−1.066 (6)
$Cu^{II}Ni^{II}L^{2+}$	−1.090	0.080	−1.092	0.100	−1.055	0.060		−1.074 (29)
$Cu^{II}Cu^{II}L^{2+}$ [21,22]	−0.930	0.070	−0.923	0.092	−0.917	0.058	1.0	−0.925 (8)
$Cu^{II}Zn^{II}L^{2+}$	−1.060	0.070	−1.060	0.100	−1.076	0.058	0.95	−1.067 (15)

[a] All measurements were taken with *N,N*-dimethylformamide as solvent and 0.1 M tetrabutylammonium perchlorate as the supporting electrolyte. Data are reported in volts vs. an internal reference, the ferrocene/ferricinium(1+) redox couple. Formal reduction potentials, $E_f(\sigma)$, represent weighted average values of measured potentials by the various techniques. [b] Formal potentials reported are $(E_{p_a} + E_{p_c})/2$. Scan rates are 0.5 V/s. Platinum button electrode was utilized as working electrodes. [c] Peak potentials measured with platinum button electrode at scan rates of 1–10 mV/s. [d] Half-wave potentials measured by using dropping mercury electrode at a scan rate of 1 mV/s. Drop time was 5 s. [e] Coulometric n values measured by electrolysis using a platinum gauze electrode. [f] Average formal potentials with one standard deviation in parentheses.

Electrochemistry. Electrochemical methods have been most effective in characterizing these complexes. The techniques utilized include cyclic voltammetry, differential pulse polarography, coulometry, and sampled DC polarography.

Electrochemical methods have helped to establish the purity of the heterobinuclear complexes. For the homonuclear complexes $M_A^{II}M_A^{II}L^{2+}$, two sequential redox processes were observed as shown in Table III. For example, for the dinuclear copper complex of L, the two sequential reductions from $Cu^{II}Cu^{II}L^{2+}$ first to $Cu^{II}Cu^{I}L^{+}$ and then to $Cu^{I}Cu^{I}L$ were observed[21] at −0.93 and −1.32 V negative of an internal reference standard,[22] the ferrocene/ferrocinium(1+) couple (Fc/Fc$^+$). In contrast, as shown in Figure 2, only a single Cu(II)/Cu(I) wave is observed in the mixed-metal copper–manganese species at −1.0 V. This indicates that only a single type of copper ion is present. The absence of shoulders at the potentials observed for the homonuclear species (Table III) indicates a less than ~5% homonuclear contaminant. The wave at ~+0.3 V (Figure 2) is the Mn(III)/Mn(II) couple and again appears without contamination. When compounds were prepared by alternate synthetic schemes to that shown in Scheme I, shoulders on the principal waves were evident to varying degrees, reaching a maximum when isomolar mixtures of pure $Fe^{II}Fe^{II}L^{2+}$ and $Cu^{II}Cu^{II}L^{2+}$ were heated at reflux for 72 h. In the latter case electrochemical analysis of products revealed an approximately statistical distribution of homo- and heteronuclear species.

The reduction potential of the Cu(II)/Cu(I) couple was determined as a function of the nature of the remote metal M_B in $Cu^{II}M_B^{II}L^{2+}$ (**1**). The results are shown in Table IV. Potentials are, within experimental error, independent of anion, the electrode (Hg or Pt), and the scan rate.

To ensure that the anion was innocent in these redox processes, we undertook a variety of experiments. All complexes with halide anions were digested with $AgClO_4$; the Cu(II)/Cu(I) reduction potentials determined in both the absence and presence of halide were identical. Addition of 100-fold excesses of tetraethylammonium chloride and bromide also confirmed the spectator role of the anion for Cu(II)/Cu(I) redox behavior. This is clearly not the case for oxidations at the M_B site. Figure 3 shows a conductometric titration of $Fe^{II}Fe^{II}L^{2+}$ with molecular bromine. After the first equivalent of bromine was added, enough to completely form $Fe^{II}Fe^{III}L^{3+}$, a sharp drop in conductivity relative to the ideal conductivity was observed in subsequent additions of bromine. The most reasonable interpretation of this behavior is that not only does bromine serve as an oxidant for Fe(II) but also, when the charge reaches a maximum in $Fe^{III}Fe^{III}L^{4+}$, the resultant bromide acts as a ligand and coordinates to one of the axial sites at the metal, resulting in the formation of appreciable amounts of $Fe^{III}Fe^{III}LBr^{3+}$. Similar behavior was observed for Mn(III) and Co(III).[12] For this reason, only the Cu(II)/Cu(I) couple was explored, fixing the remote metal at the divalent oxidation state where complications due to the anion can be avoided.

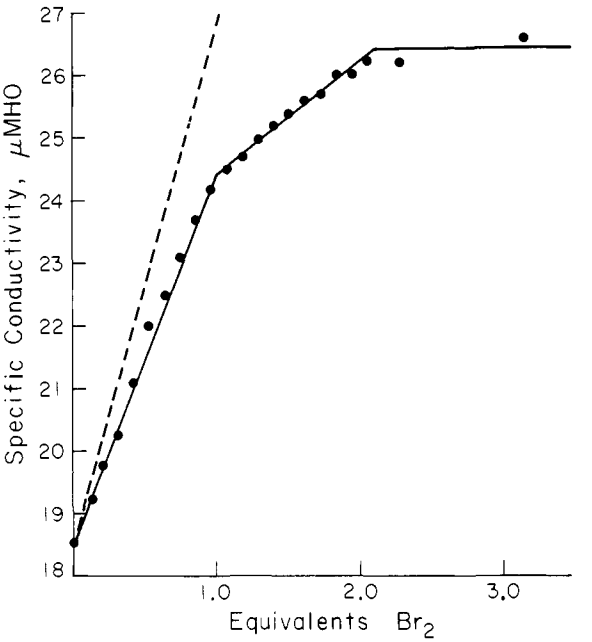

Figure 3. Conductometric titration of $Fe^{II}Fe^{II}L^{2+}$ with bromine in *N,N*-dimethylformamide. Initially the anions are completely dissociated with the species acting as a 2:1 electrolyte.[14] As bromine is added, it oxidizes the iron centers and associates with the metal ions to the extent shown by the solid line. The dashed line is the ideal behavior that would be expected for complete dissociation ultimately resulting in a 4:1 electrolyte. That the break occurs at the 1-equivalent point implies the bromide coordinates primarily with $Fe^{III}Fe^{III}L^{4+}$, forming appreciable quantities of $Fe^{III}Fe^{III}LBr^{3+}$.

When measured by cyclic voltammetry, the Cu(II)/Cu(I) redox processes were quasi-reversible to reversible. The difference, $E_{p_c} - E_{p_a}$, exceeds the Nernstian requirement of 59 mV by up to 60 mV.[23] The deviation from 59 mV is highly scan rate dependent, with slower scan rates approaching the reversibility criterion. In addition, at scan rates less than 0.1 V/s, anodic to cathodic peak currents are not equal, disproportionate loss of anodic current being observed. The reason for this is not well understood but could be due to a slow chemical reaction or rearrangement subsequent to charge transfer. Measurements of reduction potentials by differential pulse polarography yielded similar results, where potentials agreed with those measured by other techniques and are independent of scan rate. Quasi-reversible behavior was observed with this technique as well, with full widths at half

(21) R. R. Gagné, C. A. Koval, T. J. Smith, and M. C. Cimolino, *J. Am. Chem. Soc.*, **101**, 4571 (1979). C. A. Koval, Doctoral Dissertation, California Institute of Technology, Pasadena, Calif. 1978.

(22) R. R. Gagné, C. A. Koval, and G. C. Lisensky, *Inorg. Chem.*, **19**, 2854 (1980).

(23) R. S. Nicholson and I. Shain, *Anal. Chem.*, **36**, 706 (1964).

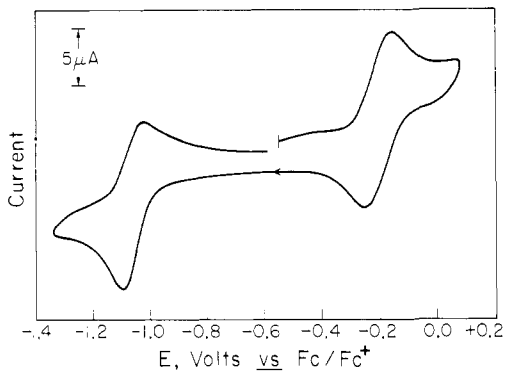

Figure 4. Cyclic voltammogram of $Cu^{II}Fe^{II}L^{2+}$. The peak at −1.058 V negative of ferrocene corresponds to the Cu(II)/Cu(I) couple in *N,N*-dimethylformamide.

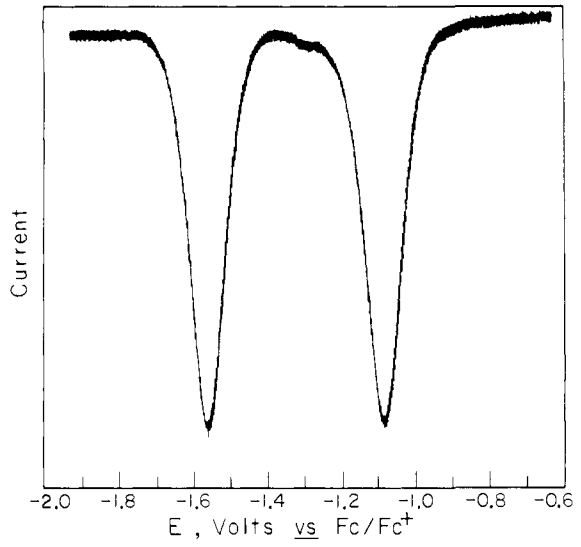

Figure 5. Differential pulse polarogram for $Cu^{II}Ni^{II}L^{2+}$. The more positive wave is the Cu(II)Cu(I) couple; the peak at −1.5 V is the Ni(II)/Ni(I) wave.

maxima (fwhm, Table IV) ranging from 92 to 120 mV. The criterion for reversibility is a 90-mV fwhm.[24] When the Cu(II)/Cu(I) processes were measured by sampled DC polarography, reversible waves were observed, showing linear plots of ln $(i_d/(i_d - i))$ with slopes of 59 ± 3 mV.[25] The values for the formal Cu(II)/Cu(I) reduction potential in Table IV represent an equally weighted average of each determination of E_f by the various techniques. Standard deviations were determined in the usual fashion. Sampled DC polarographic slopes, differential pulse peak widths, and cyclic voltammetric determinations of $E_{p_c} - E_{p_a}$ are all consistent with one-electron redox processes. Controlled potential electrolyses yielded coulometric *n* values of unity in the cases examined (Table IV).

The electrochemistry occurring at the second metal ion, M_B in $Cu^{II}M_B{}^{II}L^{2+}$, is well out of the range of redox activity at the copper site. In the case of the manganese–copper complex, a broad Mn(III)/Mn(II) wave ($E_{p_c} - E_{p_a}$ = 160 mV) is observed at ~ +0.150 V vs. Fc/Fc^+ in DMF. In methanol (Figure 2) the wave occurs at +0.300 V vs. Fc/Fc^+ and is quasi-reversible ($E_{p_c} - E_{p_a}$ = 80 mV). In *N,N*-dimethylformamide, the iron–copper binuclear complex shows a nearly reversible ($E_{p_c} - E_{p_a}$ = 80 mV) wave at −0.15 V vs. Fc/Fc^+ (Figure 4) corresponding to the Fe(III)/Fe(II) couple. In methanol, a reversible wave ($E_{p_c} - E_{p_a}$ = 60 mV) is present at +0.110 V vs. Fc/Fc^+. Current is observed for the cobalt–copper complex in the region around +0.25 V vs. Fc/Fc^+, but the wave is so broad as to offer no reasonable approximation

Table V. Equilibrium Constants, $K_{L''}$, for the Binding of Axial Bases[a]

complex	$10^{-4}K_{CO}$, M^{-1}	$K_{CH_2CH_2}$, atm^{-1}	K_{PR_3}, M^{-1}	K_{etpy}, M^{-1}
$Cu^IMn^{II}L^+$	0.9 (3)	0.3 (3)	0	22.5 (7)
$Cu^IFe^{II}L^+$	1.5 (4)	0.9 (4)	0	28 (6)
$Cu^ICo^{II}L^+$	0.9 (5)	0.3 (3)	0	10.2 (6)
$Cu^INi^{II}L^+$	1.5 (4)	0.4 (3)	4.1 (4) × 10^2	30 (4)
$Cu^ICu^{II}L^+$	3.1 (3)	1.5 (3)	1.2 (2) × 10^3	38 (14)
$Cu^IZn^{II}L^+$	1.1 (4)	1.6 (3)	0	9.7 (17)

[a] Measurements were taken as a function of the remote metal ion $M_B(II)$. Substrates (L″) studied include carbon monoxide (CO), ethylene (CH_2CH_2), tris(*o*-methoxyphenyl)phosphine (PR_3), and 4-ethylpyridine (etpy). Binding constants were determined by an electrochemical method as described in the text. Standard deviations appear in parentheses. In all cases, *N,N*-dimethylformamide containing 0.1 M tetrabutylammonium perchlorate was the solvent.

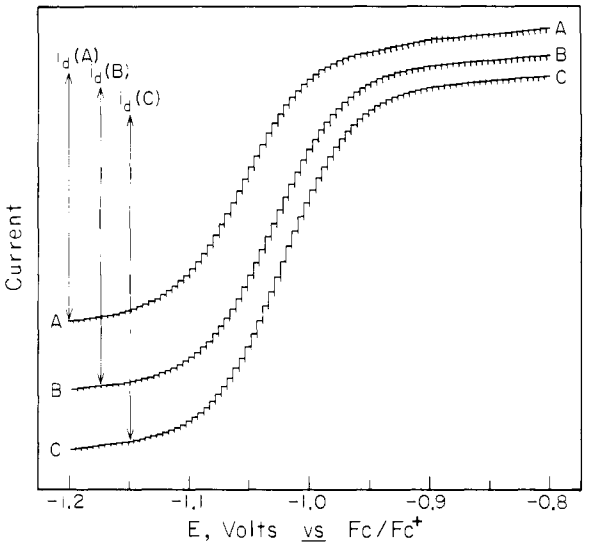

Figure 6. Polarographic determination of equilibrium binding constant for Cu(I) with tris(*o*-methoxyphenyl)phosphine in the complex $Cu^INi^{II}L^+$. The most negative wave, curve A, is the blank, while curves B and C are polarograms of $Cu^{II}Ni^{II}L^{2+}$ in the presence of 5 × 10^{-3} and 1 × 10^{-2} M phosphine, respectively. Note the positive shifts in the waves (+0.030 V for A, +0.040 V for B) indicate binding to the reduced species.

to the Co(III)/Co(II) formal potential. The nickel–copper species $Cu^{II}Ni^{II}L^{2+}$ shows two differential pulse polarographic waves (Figure 5) at −1.075 and −1.560 V vs. Fc/Fc^+. The Ni(II)/Ni(I) couple, the more negative wave, has a 70-mV peak to peak separation via cyclic voltammetry. No nickel(III)/nickel(II) couple is present prior to solvent oxidation at ca. +1.0 V. Zinc is electroinactive in the zinc–copper ion.

Chemical Studies. Ligand binding to Cu(I) as a function of the remote metal ion M_B in $Cu^IM_B{}^{II}L^+$ (**1**) (eq 1) was examined.

$$Cu^IM_B{}^{II}L^+ + L'' \overset{K_{L''}}{\rightleftharpoons} L''\text{-}Cu^IM_B{}^{II}L^+ \quad (1)$$

$$K_{L''} = \frac{[L''\text{-}Cu^IM_B{}^{II}L^+]}{[Cu^IM_B{}^{II}L^+][L'']} \quad (2)$$

Again, the remote metal (M_B) was varied across the series M_B = Mn(II), Fe(II), Co(II), Ni(II), Cu(II), and Zn(II). The results are shown in Table V. Equilibrium constants ($K_{L''}$) in eq 2 were determined via an electrochemical method which does not require the isolation of $Cu^IM_B{}^{II}L^+$ complexes. This method has been described in detail elsewhere[26,27] and is based on the principle that

(24) E. P. Parry and R. A. Osteryoung, *Anal. Chem.*, **37**, 1634 (1964).
(25) L. Meites, "Polarographic Techniques", Wiley, New York, 1965, p 218.
(26) J. L. Allison, Doctoral Dissertation, California Institute of Technology, Pasadena, Calif. 1978.
(27) R. R. Gagné, J. L. Allison, and D. M. Ingle, *Inorg. Chem.*, **18**, 2767 (1979).

binding of the axial base L″ in eq 1 depletes the concentration of $Cu^{I}M_B^{II}L^+$. Since $Cu^{I}M_B^{II}L^+$ appears in the Nernst equation, (eq 3), this decrease in the concentration $Cu^{I}M_B^{II}L^+$ due to binding

$$E_{measd} = E^\circ - \frac{RT}{nF} \ln \frac{[Cu^{I}M_B^{II}L^+]}{[Cu^{II}M_B^{II}L^{2+}]} \quad (3)$$

causes a shift in the measured potential for the Cu(II)/Cu(I) couple. For example, as can be seen in Figure 6, addition of 5×10^{-3} M of L″ = tris(*o*-methoxyphenyl)phosphine, to the nickel–copper heterobinuclear complex $Cu^{II}Ni^{II}L^{2+}$ shifts the polarographic wave due to Cu(II)/Cu(I) positive by 30 mV. By applying the Nernst expression (eq 3) to the equilibrium binding equation, we can relate this 30-mV shift in potential quantitatively to the equilibrium binding constant by the use of eq 4. In eq 4,

$$K_{L''} = \frac{e^{nF(\Delta E)/RT} - 1}{[L'']} \quad (4)$$

$$\Delta E = E_f(\text{blank}) - E_f(L'')$$

E_f(blank) is the half-wave potential measured polarographically in the absence of L″ (Table IV), while $E_f(L'')$ is the measured potential at a given concentration of L″. The other symbols have their usual meanings, with n equaling one in all cases and $K_{L''}$ representing the equilibrium constant in eq 2. In the example above for $Cu^{I}Ni^{II}L^+$, E_f(blank) = −1.055 V and $E_f(PR_3)$ = −1.025 V where $[PR_3] = 5 \times 10^{-3}$ M and $K_{PR_3} = 4.4 \times 10^2$ M^{-1}.

Use of this expression requires the usual assumption that little change in the diffusion constants takes place upon charge transfer. In addition, it requires that equilibrium be established rapidly relative to the electrochemical time scale, that the electrode surface concentration of L″ is maintained, and that no other conflicting equilibria be present.[26]

For each substrate L″ studied (L″ = carbon monoxide, ethylene, 4-ethylpyridine, and tris(*o*-methoxyphenyl)phosphine), quasi-reversible to reversible sampled DC polarograms were obtained, indicating that fast on–off equilibria had been established. All other phosphines and phosphites examined showed irreversible electrochemistry. These included triphenylphosphine, tritolylphosphines, tricyclohexylphosphine, tris(*p*-methoxyphenyl)phosphine, and a wide variety of substituted aromatic phosphites. Molecular models indicate extensive steric hindrance in the tris(*o*-methoxyphenyl)phosphine, which may play an important role in facilitating rapid establishment of equilibrium with L″.

The criterion that no other equilibria are present requires some further discussion, since these substrates may potentially bind to Cu(II) or the other M_B(II) centers in the mixed-metal species. For L″ = PR_3 and 4-ethylpyridine, a broad range of concentrations of L″ were utilized, yielding results consistent with only a single equilibrium. In addition, no shifts in the remote metal ion's wave, the M_B(III)/M_B(II) couple, were observed.[28] No spectral changes were observed in these species upon addition of bases to the oxidized form, $Cu^{II}M_B^{II}L^{2+}$, also consistent with negligible competing equilibria. Still, due to the spectral and/or electroinactivity of some of these species (i.e., Zn(II) in $CuZn^{II}L^{n+}$) contributions to the data due to binding to the oxidized form cannot be completely ruled out. In the cases where L″ = CO or ethylene (1 atm), binding to the high spin M(II) ions would be most unusual;[29] all evidence is consistent with the oxidized form being inert to these bases.

The assumption that the surface concentration of L″ at the electrode was maintained during and subsequent to charge transfer is reasonable for several reasons. A minimum tenfold excess of L″ over $Cu^{I}M_B^{II}L^+$ was utilized in all experiments, the equilibrium constants are quite small (Table V), and the equilibrium constants do not vary appreciably nor consistently over a wide range of concentrations of L″.

Discussion and Conclusions

Delocalization Energy. The binuclear copper complex $Cu^{II}Cu^{II}L^{2+}$, like many homobinuclear species, shows two sequential reductions, E_1 and E_2, separated by an amount $\Delta E = E_1 - E_2 = 0.390$ V.[21,22] The thermodynamic significance of ΔE can be illustrated by the comproportionation equilibrium shown in eq 5 and 6. A large value of ΔE indicates a considerable

$$Cu^{II}Cu^{II}L^{2+} + Cu^{I}Cu^{I}L \overset{K_{com}}{\rightleftharpoons} 2Cu^{II}Cu^{I}L^+ \quad (5)$$

$$\Delta E = RT/nF \ln K_{com} \quad (6)$$

stability of the mixed-valent $Cu^{II}Cu^{I}L^+$ ion relative to its constituents, the equilibrium lying far to the right in eq 5.

In general K_{com} reflects a number of microscopic phenomena. (I) Major structural changes such as bond making and breaking, changes in coordination number, and severe changes in corrdination geometry upon charge transfer can shift comproportionation equilibria.[30] (II) If no interaction takes place between the metal ions, $K = 4$, on the basis of statistical distribution of charges, resulting in a ΔE value of 0.036 V and a single voltammetric wave.[31] (III) If the metal ions are in close proximity, a through-space coulombic interaction may be important. A $n+$ ion will be more readily reduced than a $(n+) - 1$ ion on the basis of electrostatic considerations alone. This will increase ΔE and hence K_{com}. (IV) Magnetic superexchange effects between two metals may stabilize one or more oxidation states in species which contain multiple paramagnetic centers, also resulting in a change in ΔE. (V) Electronic delocalization in mixed oxidation states will enhance the stability of these species with resulting increases in ΔE.

The heteronuclear complexes $M_A^{II}M_B^{II}L^{2+}$ (**1**), were examined to help quantitatively define some of these effects. The complexes were designed to (I) minimize structural effects accompanying redox changes, (II) keep coulombic interactions constant and cancelable, and (III) permit superexchange effects to be measured separately. It was expected that electrochemical measurements would then enable a determination of electronic delocalization energies in mixed-valent species. In fact, this approach worked well for the complexes $Cu^{II}M_B^{II}L^{2+}$ (**1**), for which the Cu(II)/Cu(I) reduction potential was determined as a function of the remote metal ion M_B(II). The results, summarized in Table IV, are unequivocal. Within experimental error, the Cu(II)/Cu(I) reduction potentials are independent of the remote metal ion M_B, unless M_B is copper(II). For $M_A = M_B$ = Cu(II), it is easier to add an electron by an average of 143 (14) mV or 3.3 (3) kcal/mol. We ascribe this difference in $Cu^{I}Cu^{II}L^+$ vs $Cu^{I}M_B^{II}L^+$ ($M_B \neq$ Cu) to the fact that only the $Cu^{I}Cu^{II}L^+$ species can exist, to any extent, as a resonance-stabilized, delocalized ion. The electronic delocalization energy in $Cu^{I}Cu^{II}L^+$ is the major contribution to the 3.3 (3)-kcal/mol value, as can be shown by more detailed analysis of the experimental data and the factors affecting the redox properties of these particular complexes, as follows.

Although the macrocyclic ligand in $CuM_B^{II}L^{n+}$ can accommodate a range of coordination geometries,[10-13] it is likely that only negligible structural changes accompany one-electron reduction of $Cu^{II}M_B^{II}L^{2+}$. While conductivity studies along with electrochemical experiments cited in the Results clearly demonstrate that the anion exhibits the potentiality to bind to higher oxidation states of metals complexed with L, they also indicate the spectator role of the anion in Cu(II)/Cu(I) redox behavior. Indeed for this reason, the decision to study Cu(II)/Cu(I) electrochemistry as a function of the remote metal was made. It is possible, however, that the solvent may be involved in some fluxional manner with the copper center. While it is unreasonable

(28) One exception is the Mn(III)/Mn(II) wave in the presence of high concentrations (>0.1 M) of ethylpyridine, when the wave obliterated. At low concentrations of ethylpyridine, the Mn(III)/Mn(II) wave is unchanged. Equilibrium constants, $K_{L''}$, were determined at low concentrations where only a slight error may be introduced due to K(II), the binding to Mn(II).

(29) The lack of affinity for CO by Fe(II) may appear somewhat surprising, but all attempts to prepare complexes of this type were unsuccessful.

(30) J. Phelps and A. J. Bard, *J. Electroanal. Chem.*, **68**, 313 (1976). R. E. Dessy, P. M. Weissman, and R. L. Pohl, *J. Am. Chem. Soc.*, **88**, 5117 (1966). N. H. Furman and G. Stone, *J. Am. Chem. Soc.*, **70**, 3055 (1948).

(31) Michael Flanagan, Doctoral Dissertation, California Institute of Technology, Pasadena, Calif. 1978.

to suggest that there will be no changes in the coordination geometry at copper upon charge transfer, it is likely that whatever changes occur in the reduced form (e.g., a distortion toward tetrahedrality) do so in such a uniform across the series $M_B(II)$ = Mn(II), Fe(II), Co(II), Ni(II), Cu(II), and Zn(II) as to obviate the need for concern here. The concordance of the data supports such an assumption. While the geometry at the $M_B(II)$ site in solution is unknown, it is unlikely that significant changes in coordination occur at $M_B(II)$ upon charge transfer to Cu(II).

The statistical contribution of ΔE of 36 mV (K_{com} = 4) holds for identical, noninteracting metal ions. As metal–metal interaction increases, the statistical contribution is expected to decrease. For $Cu^{I}Cu^{II}L^{+}$, in which significant interaction is apparent (vide infra), only a very small, essentially negligible, statistical contribution is expected.[31]

Coulombic contributions to the Cu(II)/Cu(I) reduction potential in $CuM_B^{II}L^{n+}$ are essentially constant since the 2+ charge on M_B and, most likely, the Cu to $M_B(II)$ distance (~3.15 Å)[10-13] are maintained for all $M_B(II)$. This hypothesis is supported by the data in Table IV. Although the Cu(II)/Cu(I) reduction potentials are surely dependent on the charge of the remote metal, M_B, constant values of E_f(Cu(II)/Cu(I)) were observed for all $M_B(II) \neq Cu(II)$, within experimental error.

The contribution to ΔE due to magnetic superexchange is more complex. In the dicopper ion $Cu^{II}Cu^{II}L^{2+}$, J = −293 cm^{-1},[19] where $2J$ represents the singlet–triplet splitting. The coupling drops off rapidly for the other heteronuclear species.[20] The dicopper ion is a singlet–triplet system, with each spin state S having an associated reduction potential ^{S}E. Since the singlet represents the more stable ground state, it will have a more negative reduction potential than for the triplet. In both cases, the reduced species is the same since no spin coupling is possible.

To compare the potential in the binuclear copper complex to that of the heteronuclear species, we need the potential for the copper complex for J = 0. This potential, E, for J = 0 was calculated from the observed potential (E_f = −0.925 V vs. Fc/Fc$^+$) and the singlet–triplet separation, as follows.

(1) It was assumed that the distribution of spin states at the electrode was constant throughout the course of charge transfer. This is reasonable in light of the rapid kinetics of spin interconversion observed in spin-equilibria systems.[32] On the basis of a Boltzmann distribution, 15% of the ions are in the triplet state with the remaining 85% in the singlet state, a distribution that is independent of the electrode potential.

(2) A single reduction wave is expected and was observed, due to the rapid spin interconversion. Since the singlet–triplet separation is appreciable (586 cm^{-1}; $^{3}E - {}^{1}E$ = 73 mV), the triplet ion is the principal species reduced. As it is reduced, its depleted concentration at the electrode surface is replenished rapidly to maintain spin state equilibrium.

(3) The triplet reduction potential, ^{3}E, was calculated from the observed potential, E_{obsd}, by using the Nernst equation

$$E_{obsd} = {}^{3}E - \frac{RT}{nF} \ln \frac{[^{3}(Cu^{II}Cu^{II}L^{2+})]}{[Cu^{II}Cu^{I}L^{+}]}$$

For $[^{3}(Cu^{II}Cu^{II}L^{2+})]$ which is 15% of the total $[Cu^{II}Cu^{II}L^{2+}]$ with E_{obsd} = −0.925 V, then ^{3}E = −0.876 V and, correspondingly, ^{1}E = −0.949 V.

(4) In the limit of J = 0 these potentials converge to a value three quarters of the way toward the singlet at −0.931 V, which is a consequence of the degeneracy in the triplet state. This is manifest in the equation[33] $^{S}\epsilon = -J(S(S+1) - s_1(s_1+1) - s_2(s_2+1))$, the solution to the isotropic Heisenberg Hamiltonian $\hat{\mathcal{H}} = -J(\hat{S}_1 - \hat{S}_2)$, ($S$ = 1 or 0, $\hat{s}_1 = \hat{s}_2 = {}^{1}/_{2}$, $^{3}\epsilon = {}^{1}/_{2}J$, $^{1}\epsilon = -{}^{3}/_{2}J$).

The difference between the observed potential (E_{obsd} = −0.925 V vs. Fc/Fc$^+$) and the corrected potential ($E_{J=0}$ = −0.931 V) is

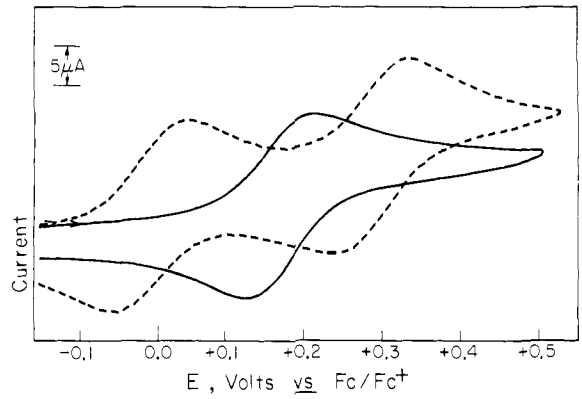

Figure 7. Cyclic voltammograms of $Cu^{II}Fe^{II}L^{2+}$ (solid line) and $Fe^{II}Fe^{II}L^{2+}$ in methanol. Note that the Fe(III)/Fe(II) couple occurs at a more positive potential in $Cu^{II}Fe^{II}L^{2+}$ than in $Fe^{II}Fe^{II}L^{2+}$.

6 mV. For the heteronuclear species J is still smaller and thus the magnetic contribution was ignored.

The corrected reduction potential for $Cu^{II}Cu^{II}L^{2+/+}$ (E_{corr} = −0.931 V) accounts for structural, Coulombic, entropic, and magnetic contributions to E_f, as explained above. The difference in E_{corr} and the mean Cu(II)/Cu(I) reduction potential in $Cu^{II}M_B^{II}L^{2+}$ (E = −1.068 V) is 137 mV. This 137 mV = 3.2 kcal/mol can be ascribed to the special stability associated with a degree of electronic delocalization in the mixed-valent $Cu^{I}Cu^{II}L^{+}$ ion. This delocalization stabilization may represent one or more phenomena including (a) covalent effects, wherein the single unpaired electron occupies a stabilized three center molecular orbital, (b) simple charge redistribution within the complex, decreasing internuclear and interelectronic repulsion, and (c) greater solvation of the delocalized state $(Cu^{1.5+}Cu^{1.5+}L)^{+}$ relative to the completely localized ion $(Cu^{1+}Cu^{2+}L)^{+}$.

That mixed-valent $Cu^{I}Cu^{II}L^{+}$ ion experiences significant delocalization is supported by previous studies of this molecule[21] which demonstrated the presence of a delocalized seven-line hyperfine pattern in the ESR spectrum, as well as an intervalence, or metal-to-metal charge-transfer band in the electronic spectrum. It is unlikely that electron transfer from Cu(I) to $M_B(II)$ will occur for any other metal, since the transfer of charge from Cu(I) to $M_B(II)$ would require surmounting a minimum barrier of 10 kcal/mol in the case where M_B = Ni(II) and may be very large for M_B = Zn(II).

Similar delocalization may also occur in related mixed-valent complexes, $M_B^{II}M_B^{III}L^{3+}$, as revealed by a consistent pattern in $M_B(III)/M_B(II)$ redox couples in $M_B^{II}M_B^{II}L^{2+}$. It appears easier to effect the first oxidation of $M_B(II)$ in the homonuclear complexes $M_B^{II}M_B^{II}L^{2+}$ (Table III) than in $Cu^{II}M_B^{II}L^{2+}$. In light of the Cu(II)/Cu(I) data, a special stability might be expected for $M_B^{II}M_B^{III}L^{3+}$. In particular, the oxidation $Mn^{II}Mn^{II}L^{2+} \rightarrow Mn^{II}Mn^{III}L^{3+}$ occurs at −0.05 V vs. ferrocene compared to +0.300 V for $Cu^{II}Mn^{II}L^{2+} \rightarrow Cu^{II}Mn^{III}L^{3+}$, though in the former the manganese(III)/manganese(II) couple is strongly anion dependent ranging from −0.05 V (X = Br$^-$) to −0.02 V (X = OAc$^-$) to +0.03 V (X = ClO_4^-). In any case, the first M(III)/Mn(II) oxidation of the homonuclear complex does appear to always be negative of that for the heteronuclear complex (X = Cl$^-$) consistent with the copper(II)/copper(I) trend. Similarly, comparison of the first Fe(III)/Fe(II) oxidation in $Fe^{II}Fe^{II}L^{2+}$ vs. that in $Cu^{II}Fe^{II}L^{2+}$ (Figure 7) reveals that the mixed-valent $Fe^{II}Fe^{III}L^{3+}$ is more accessible (by 130 mV = 3.3 kcal/mol than is $Cu^{II}Fe^{III}L^{3+}$. While no clean cobalt(III)/cobalt(II) electrochemical processes were observed in $Cu^{II}Co^{II}L^{2+}$, current was observed approximately 250 mV positive of the first Co(III)/Co(II) oxidation in $Co^{II}Co^{II}L^{2+}$, again consistent with the observed trend in the dinuclear copper ion. In each case, the species which exhibits the structural potentiality for delocalization is the most thermodynamically accessible. It cannot be overemphasized, however, that these latter results may be fortuitous and artifactual since structural controls have been relaxed, on the basis of the known propensity of trivalent

(32) E. V. Dose, M. A. Hoselton, N. Sutin, M. F. Tweedle, and L. J. Wilson, *J. Am. Chem. Soc.*, **100**, 1141 (1978).

(33) This is in contrast to a previously reported calculation due to magnetic exchange.[15] The authors are grateful to Dr. Charles Dismukes, Princeton University, for pointing this out.

metal ions bound to L to coordinate anions to varying degrees (Figure 3). In addition no extensive study such as that for the mixed-metal series, $Cu^{II}M_B^{II}L^{2+}$, has been undertaken as a control nor has any evidence for delocalization in the $M_B^{II}M_B^{III}L^{3+}$ series been demonstrated.

Our interpretation of these results may shed some light on previously reported electrochemical data in other systems which show a propensity toward electronic delocalization. In mixed-valent systems which have a completely delocalized ground state, class III in the Robin and Day scheme,[34] unusually large values of K_{com} and ΔE have been observed. For example, the oxo-bridged binuclear ruthenium complexes, $(NH_3)_5Ru$–O–$Ru(NH_3)_5^{5+}$ [35] and $(bpy)_2Cl$–Ru–O–$Ru(bpy)_2Cl^{3+}$,[36] exhibit ΔE values of 2.0 V (K_{com} = 10^{34}) and 2.2 V (K_{com} = 10^{38}), respectively. We suggest that such extraordinarily large values of K_{com} are primarily due to the special stability of delocalized ions ($Ru^{III}Ru^{IV}$) relative to the fully oxidized ($Ru^{IV}Ru^{IV}$) and fully reduced ($Ru^{III}Ru^{III}$) species. Another system which exhibits delocalization is the mixed-valent $(NH_3)_5Ru$–pyrazine–$Ru(NH_3)_5^{5+}$ [37] ion reported by Creutz and Taube.[38] The reported Ru(III)/Ru(II) reduction potentials for $Ru^{III}Ru^{III} \rightarrow Ru^{II}Ru^{III} \rightarrow Ru^{II}Ru^{II}$ are E_1 = +0.700 V and E_2 = +0.310 V, giving ΔE = 0.39 and $K_{com} = 4 \times 10^6$. The Ru(III)/Ru(II) reduction potential in the Ru–Rh analogue $(NH_3)_5Ru$–pyrazine–$Rh(NH_3)_5^{6+/5+}$ was also reported (E_1 = 0.650 V). We propose that the difference of 50 mV = 1.2 kcal/mol between E_1 for the Ru–Ru vs. the Ru–Rh complex is another manifestation of the delocalization phenomenon, where the Ru(III)–Ru(II) species can have a delocalized ground state, while the electron is clearly trapped at ruthenium in the Ru(II)–Rh(III) dimer. Additional supportive evidence for the generality of this phenomenon is exhibited by **2** vs **3**. For **2**, K_{com}

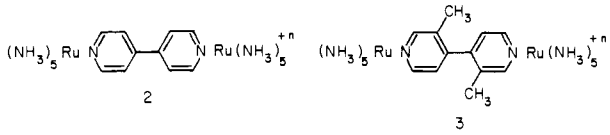

= 20 while complex **3** has K_{com} = 10;[39] in **3** the dimethyl substitution probably results in a dihedral twist between the pyridyl planes, a steric effect which may block the conjugated pathway, and hence delocalization between the metals.

In seeking to understand polymetallic enzymes and catalysts, especially those involved in redox transformations, it is important to recognize that mixed-valent moieties may represent special pockets of stability. In some cases nature may have utilized these thermodynamic sinks to adjust reduction potentials. For example, in high potential iron proteins with cubane type Fe_4S_4 groups extensive delocalization in the mixed-valent species has been demonstrated[40] and is likely to be one reason these clusters have such a large range of potentials. Elsewhere, such as in electrocatalysts to be utilized for multielectron reactions, this delocalization energy could cause sequential rather than concerted charge transfers, resulting in significant overpotentials and loss of catalyst efficiencies.

Ligand Binding. In addition to redox coupling between metals, the chemical manifestations of metal–metal interactions have been probed by studying the equilibria

$$Cu^{I}M_B^{II}L^{+} + L'' \rightleftharpoons Cu^{I}(L'')M_B^{II}L^{+}$$

The data are summarized in Table V. Note that small incremental changes in equilibrium constants represent very small differences in ΔG. For weakly binding bases such as ethylene or 4-ethylpyridine any significant variations in binding parameters have been lost in the experimental noise. In contrast, chemical binding constants for tris(*o*-methoxyphenyl)phosphine and for carbon monoxide are large and differences in these series appear to be significant.

In light of the electrochemical data summarized in Table IV which indicated that the heterometal ion M_B(II) has little effect on the electron density at the copper site, the results on the chemical consequences (Table V) of metal–metal interactions are somewhat surprising. No obvious trends are present in this limited study, but some predictions are clearly not borne out. First, *the chemical binding of axial bases L'' to Cu(I) is not independent of the heterometal*, as the redox potentials might imply. Second, we might have expected that the axial bases would bind more poorly to the dinuclear copper species relative to the others, since this would likely result in some loss of electronic delocalization by introducing an inequivalence to the metals. This was also not observed. In any case, it is apparent that the chemical manifestations of metal–metal interactions do not represent a simple reflection of their redox properties but are a complicated function of several as yet undetermined factors. Though these results are poorly understood, it is both encouraging and exciting that some chemical manifestation that is dependent on the nature of the heterometal ion has been discovered. Obviously, more extensive experimental studies accompanied by a firm theoretical basis are needed to determine the generality and significance of this observation.

Experimental Section

Physical Measurements. Infrared spectra were taken as Nujol mulls by using a Beckmann IR4240 model grating infrared spectrophotometer. Electronic absorption spectra were measured by using a Cary 14 model UV/visible spectrophotometer. Magnetic measurements were made via the Faraday method, at the ambient temperature by using a Cahn electrobalance, or by a vibrating magnetometer as described elsewhere.[41] Magnetic moments were corrected for diamagnetism by using Pascal's constants.[42] Elemental analyses were performed by the California Institute of Technology analytical facility along with Galbraith Microanalytical Laboratories, Knoxville, Tenn. Absolute metal percentages were determined by atomic absorption. Metal ratios were conveniently determined by the integral counting of back-scattered X-ray fluorescence radiation from an International Scientific Instruments SMS 2-2 model scanning electron microscope, equipped with a Tracor Northern Model TN-1700 data processor.

Electrochemical data were taken with a Princeton Applied Research Model 174A Polarographic Analyzer in the cyclic voltammetric (CV), differential pulse polarographic (DPP), and sampled DC (SDC) polarographic modes. Platinum button electrodes were used in the CV and DPP modes, with the dropping mercury electrode used in the SDC mode. In the latter case, drop times were restricted to 5 s, though scan rates varied from 0.2 to 1.0 mV/s. Coulometric measurements were performed on a Princeton Applied Research Model 173 digital coulometer by using a platinum gauze electrode for oxidations and a mercury pool electrode for reductive electrolyses. The cell components consisted of a standard two compartment cell with the chambers separated by medium porosity sintered glass. One compartment housed the working electrode, the auxiliary electrode (Pt wire), and the electroactive solution. The other chamber contained a Ag/Ag^+ reference electrode (Ag wire/$AgNO_3$, 0.01 N in acetonitrile) to complete the circuit. In actuality, the reference electrode was not used to determine reduction potentials. Rather, an internal standard, the ferrocene/ferricinium(1+) couple was utilized. In each case, a small amount of ferrocene was added to the electroactive solution for comparison to the measured potentials. This method, described in detail elsewhere,[22] enables us to circumvent any temporal variations in junction potentials or ohmic drop due to uncompensated solution resistance. All solutions were saturated with an inert gas for at least 15 min prior to analysis.

Synthesis of Compounds. All solutions and reagents were purchased from commercial sources and utilized without further purification. One exception is the *N,N*-dimethylformamide (DMF) used as an electrochemical solvent, which was distilled over molecular sieves and anhydrous $MgSO_4$ prior to use.

(34) M. B. Robin and P. Day, *Adv. Inorg. Chem. Radiochem.*, **10**, 247 (1967).
(35) J. A. Bauman and T. J. Meyer, *Inorg. Chem.*, **19**, 345 (1980).
(36) T. R. Weaver, T. J. Meyer, S. Adeyemi, G. M. Brown, R. P. Eckberg, E. C. Johnson, R. W. Murray, and D. Untereker, *J. Am. Chem. Soc.*, **97**, 3039 (1975).
(37) J. H. Elias and R. S. Drago, *Inorg. Chem.*, **11**, 415 (1972).
(38) C. Creutz and H. Taube, *J. Am. Chem. Soc.*, 95, 1086 (1973).
(39) James P. Sutton, Doctoral Dissertation, Stanford University, Stanford, Calif., 1979.
(40) C. Y. Yang, K. H. Johnson, R. H. Holm, and J. B. Norman, Jr., *J. Am. Chem. Soc.*, **97**, 6596 (1975).
(41) See, for example, ref 19.
(42) A. Earnshaw, "Introduction to Magnetochemistry", Academic Press, London, 1968, pp 9–12.

2,6-Diformyl-5-methylphenol.[43] *p*-Cresol (216 g) was added to a solution of NaOH (100 g) in water (400 mL). Following full development of a gold color, 37% formaldehyde (430 g) was added. The mixture was stirred for 20 min and allowed to stand overnight at the ambient temperature. The yellow granular 2,6-dimethylol-5-methylphenol product was collected by vacuum filtration and washed with water-saturated sodium chloride (2 × 400 mL). This product was transferred to a 3-neck, 5-L round-bottom flask fitted to an overhead stirrer. Water (1300 mL) and a 33% sodium hydroxide solution (130 mL) were added. The mixture was stirred for ~0.5 h. *p*-Toluenesulfonyl chloride (494 g) dissolved in toluene (520 mL) was added, and the solution was allowed to stir for 20 h, at which time an aqueous and emulsified phase were present. The mixture was cooled in an ice–water bath, and toluene (200 mL) was added with stirring. After 10 min, additional toluene (300 mL) was added, at which point solids were evident. After 1 h, a final amount of toluene (100 mL) was added. This slurry was stirred for 15 min, at which time the white solid tosylated derivative was collected by vacuum filtration, washed with toluene (400 mL), and dried under vacuum for 12 h or until the drying was judged complete. The white solids were weighed and transferred to a 5-L, 3-neck round-bottom flask equipped with an overhead stirrer, a water-cooled reflux condensor, and a 125-mL addition funnel. Acetic acid (14 mol/mol of tosylated phenol) and sodium dichromate (1 mol/mol of the tosylated phenol, fw = 338) were required for the oxidation, as follows. Approximately one-fourth of the acetic acid was added to the tosylated phenol in the 5-L flask. The mixture was heated to reflux with stirring (110–116 °C). The remaining acetic acid was added to the dichromate in a 2-L beaker, with dissolution accomplished by heating on a steam bath. The dichromate/acid solution was added dropwise with stirring to the tosylated phenol over 35 min. *Caution*! strong oxidant. After addition was complete, stirring at reflux was continued for 10 min. The solution was then allowed to cool slowly (~3 h) to the ambient temperature. The crystals which had formed were collected with vacuum filtration and washed with water until most of the green color was gone, leaving a pale green solid. The product was vacuum dried overnight. The dry tosylated dialdehyde (~285 g) was added slowly to concentrated sulfuric acid (900 mL) in a 4-L beaker, and the solution was stirred for 1 h. The beaker was placed in an ice bath. An ice-water slurry was added slowly to the acid solution until the total volume reached 3800 mL. After all the ice melted, the precipitate was collected by vacuum filtration, washed with water (3 × 250 mL), and dried overnight. The crude product was recrystallized from toluene, yielding pale brown needles (95 g, 29% overall yield) which were used without further purification. A more pure product can be obtained by sublimation. *Caution*! Skin contact with 2,6-diformyl-4-methylphenol leaves a deep yellow stain which will persist for several days. The melting point was 129–130 °C (lit. 133.5 °C). The NMR spectrum, showing singlets at 11.4 (phenolic), 10.2 (aldehydic), 7.8 (aromatic), and 2.4 ppm (methyl), is consistent with that of the assigned structure.

$Cu^{II}L'$.[17] To warm *N,N*-dimethylformamide (40 °C, 50 mL) containing 2,6-diformyl-4-methylphenol (1.950 g) was added 1,3-diaminopropane (0.5 mL) dropwise, with stirring, followed by the addition of solid cupric acetate (1.183 g of $Cu(OAc)_2 \cdot 2H_2O$). The warm solution was allowed to stir until all the turquoise crystals of copper acetate had dissolved. At this point, deep olive green needles of CuL' had formed. These were collected within 0.5 h, washed with diethyl ether, and vacuum dried.

Anal. Calcd: C, 58.74; H, 4.66; N, 6.52. Obsd: C, 58.5; H, 4.7; N, 6.75.

$Ni^{II}L'$. The preparation is identical with that of $Cu^{II}L'$, excepting that nickel acetate (1.475 g of $Ni(OAc)_2 \cdot 4H_2O$) was substituted for cupric acetate. The resulting crystals were yellow-brown.

Anal. Calcd: C, 59.43; H, 4.71; N, 6.60. Obsd: C, 59.75; H, 4.9; N, 6.7.

$Cu^{II}Mn^{II}L'Cl_2$. To methanol (30 mL under helium atmosphere at the ambient temperature was added manganous chloride (2.0 g $MnCl_2 \cdot 6H_2O$). To this solution was added solid $Cu^{II}L'$ (2.09 g). This was stirred until the resulting green solids appeared homogeneous but in no case for more than 10 min. The product was collected by vacuum filtration, washed with diethyl ether, and vacuum dried.

$Cu^{II}Mn^{II}LCl_2 \cdot H_2O$. To methanol (30 mL) at the ambient temperature under a helium atmosphere was added $Cu^{II}Mn^{II}L'Cl_2$ (2.32 g). 1,3-Diaminopropane (0.33 mL) was added dropwise with stirring. Within 5 min brownish green crystals had formed and were collected, washed with diethyl ether, and vacuum dried.

Anal. Calcd: C, 47.2; H, 4.6; N, 9.2; Cu, 10.3; Mn, 9.1. Obsd: C, 46.8; H, 4.4; N, 8.7; Cu, 9.8; Mn, 9.5.

$Cu^{II}Fe^{II}L'Cl_2 \cdot 2H_2O$. To methanol (30 mL) at the ambient temperature under a helium atmosphere was added $Cu^{II}L'$ (0.5 g). Ferrous chloride (0.233 g of $FeCl_2 \cdot 4H_2O$) was added to this solution with stirring until the formation of deep purple crystals was judged complete, ~10 min. These were collected, washed with diethyl ether, and vacuum dried. Addition of diethyl ether to the filtrate resulted in the formation of additional product.

Anal. Calcd: C, 42.71; H, 4.06; N, 4.74. Obsd: C, 43.1; H, 3.9; N, 4.45.

$Cu^{II}Fe^{II}LCl_2 \cdot H_2O$. To methanol (20 mL) at the ambient temperature under a helium atmosphere was added $Cu^{II}Fe^{II}L'Cl_2 \cdot H_2O$ (0.576 g). 1,3-Diaminopropane (0.068 mL in 1.0 mL of methanol) was added dropwise with stirring. Within 5 min orange crystals had formed and were collected, washed with diethyl ether, and vacuum dried.

Anal. Calcd: C, 47.2; H, 4.6; N, 9.2; Fe, 9.2; Cu, 10.3. Obsd: C, 47.6; H, 4.6; N, 9.3; Fe, 9.1; Cu, 10.4.

$Cu^{II}Co^{II}L'Cl_2 \cdot 2H_2O$. To methanol (20 mL) at the ambient temperature under a helium atmosphere was added cobaltous chloride ($CoCl_2 \cdot 6H_2O$, 2.0 g recrystallized from H_2O). To this was added $Cu^{II}L'$ (2.0 g) as a solid. After the solution was stirred for ~10 min, an emerald green microcrystalline solid had formed and was collected, washed with diethyl ether, and vacuum dried.

Anal. Calcd: C, 43.8; H, 3.8; N, 4.9. Obsd: C, 43.3; H, 4.3; N, 4.6.

$Cu^{II}Co^{II}LCl_2 \cdot H_2O$. To methanol (15 mL) at the ambient temperature under a helium atmosphere was added $Cu^{II}Co^{II}L'Cl_2 \cdot H_2O$ (1.0 g). 1,3-Diaminopropane (0.13 mL in 1.0 mL of methanol) was added dropwise with stirring. Within 10 min olive green crystals had formed and were collected, washed with diethyl ether, and vacuum dried. The copper–cobalt binuclear seems much more soluble than the other heterobinuclear species reported herein. For this reason, considerable care should be exercised in keeping solution volumes to a minimum in this synthesis.

Anal. Calcd: C, 47.0; H, 4.6; N, 9.1; Co, 9.6; Cu, 10.3. Obsd: C, 47.0; H, 5.0; N, 9.0; Co, 9.2; Cu, 10.4.

$Ni^{II}Cu^{II}L'Cl_2 \cdot 3H_2O$. Hydrated cupric chloride (2.0 g of $CuCl_2 \cdot 4H_2O$) was dissolved in methanol (40 mL) at the ambient temperature in air. Solid $Ni^{II}L'$ (1.7 g) was added with stirring. Within 10 min a golden brown microcrystalline solid was collected, washed with diethyl ether, and vacuum dried.

Anal. Calcd: C, 40.00; H, 4.45; N, 4.45. Obsd: C, 40.35; H, 4.25; N, 4.25.

$Cu^{II}Ni^{II}LCl_2 \cdot 2H_2O$. In methanol (30 mL) in air at the ambient temperature was added $Ni^{II}Cu^{II}L'Cl_2 \cdot 3H_2O$ (1.0 g). A solution of methanol (1.0 mL) containing 1,3-diaminopropane (0.13 mL) was added dropwise with stirring. The solution first turned greenish yellow, and within ca. 5 min, an emerald green solid had formed. This was collected, washed with diethyl ether, and vacuum dried.

Anal. Calcd: C, 45.6; H, 4.8, N, 8.9; Cu, 10.0; Ni, 9.4. Obsd: C, 45.8; H, 4.7; N, 8.8; Cu, 10.0; Ni, 10.0.

$Cu^{II}Zn^{II}L'(ClO_4)_2 \cdot 2H_2O$. To methylene chloride (10 mL) at the ambient temperature in air was added CuL' (0.1 g). A solution of tetrahydrofuran (6 mL) containing $Zn(ClO_4)_2 \cdot 6H_2O$ (0.18 g) was added to the CH_2Cl_2 solution slowly with stirring. Within 20 min, light green solids were present. After the solution was cooled on an ice bath for ~0.5 h, the powder was collected, washed with THF (15 mL), and vacuum dried.

Anal. Calcd: C, 34.64; H, 3.32; Cu, 8.73. Obsd: C, 34.77; H, 3.43; Cu, 8.53.

$Cu^{II}Zn^{II}L(ClO_4)_2 \cdot 2H_2O$. To tetrahydrofuran (8 mL) at the ambient temperature in air was added $Cu^{II}Zn^{II}L'(ClO_4)_2 \cdot 2H_2O$. 1,3-Diaminopropane (0.01 mL) was added dropwise with stirring to the green suspension. Stirring was continued for 20 min, at which time the solution was cooled on an ice bath. The green powder was collected by vacuum filtration, washed with THF (2 × 10 mL), and vacuum dried.

Anal. Calcd: C, 37.61; H, 3.95; Cu, 8.29. Obsd: C, 38.88; H, 4.35; Cu, 7.92.

Acknowledgment. We appreciate financial assistance from the National Science Foundation (Grant No. CHE79-27141) and a Sloan Fellowship to R.R.G.

(43) F. Ullmann and K. Brittner, *Chem. Ber.*, **42**, 2539 (1909).